

PHYSICAL PROPERTIES AND DETECTION OF SATURN'S LIGHTNING RADIO BURSTS

P. Zarka^{*}, B. Cecconi^{*,¶}, L. Denis[†], W. M. Farrell[‡], G. Fischer[§],
G. B. Hospodarsky[¶], M. L. Kaiser[‡], and W. S. Kurth[¶]

Abstract

Physical properties of Saturn's lightning radio bursts (occurrence, duration, flux, spectrum) are derived from Cassini-RPWS observations and compared to Voyager results. During the active storm of September 2004, peak occurrence rates, durations and spectral power were similar to those measured by Voyager. However, long-term occurrence appears very variable. Evidence is found for ionospheric propagation effects (cutoff and refraction), confirming the atmospheric origin of the observed bursts. The most intense ones should be detectable from the ground with presently available low-frequency radiotelescopes. Observation techniques are discussed together with preliminary results.

1 Lightning detection and occurrence

Nearly 24 years after the first Voyager-Saturn flyby which led to the discovery of Saturn's lightning [Warwick et al., 1981; Kaiser et al., 1983], Cassini is performing long-term monitoring of these atmospheric emissions. We address here their physical properties as derived by the high frequency receiver (HFR) of the RPWS investigation [Gurnett et al., 2004]. Lightning radio emission consists of brief broadband bursts. When observed with a swept-frequency receiver this emission is detected as burst segments of apparent bandwidth Δf (the band swept during the occurrence of the burst) randomly distributed over the total true spectrum of the bursts. For the present study, automated detection over long intervals was performed by comparing each measurement with its immediate neighbours recorded with the same instrument status (frequency, antenna selection), and retaining measurements with intensity $> x$ dB above these neighbours. In a second pass, fixed frequency interference and spurious broadband interference were automatically

^{*} *Observatoire de Paris, LESIA, UMR CNRS 8109, 92195 Meudon, France*

[†] *Station de Radioastronomie, CNRS-Observatoire de Paris, Nançay, France*

[‡] *NASA Goddard Space Flight Center, Greenbelt, MD, USA*

[§] *Space Research Institute, Austrian Academy of Sciences, Schmiedlstrasse 6, A-8042 Graz, Austria*

[¶] *Dept. of Physics and Astronomy, University of Iowa, Iowa City, IA 52242, USA*

eliminated on the basis of their non random distribution in the time-frequency (t-f) plane. No ‘visual’ confirmation event by event was done here. The interval from 2004/01/01 (6 month prior to insertion in orbit) to 2005/03/31 is studied here, with a detection threshold $x = 1$ dB. We restricted frequencies to above 1.8 MHz (high-frequency band of the HFR). The RPWS/HFR is run in a number of specific modes of observation adapted to specific radio components. This powerful capability is also a difficulty when performing long-term statistics on the data. Due to the variable instrument setup, a relative threshold of 1 dB corresponds to a variable number of standard deviations of the background noise (thus to a variable effective S/N). Figure 1a illustrates this variable effective S/N threshold between < 2 and > 5 as a function of time over the period studied (the first 90 days of 2005 correspond to DOY 2004 367 to 457). Figure 1b shows the fraction of the time spent by the HFR dwelling at frequencies > 1.8 MHz. Figure 2 displays the occurrence

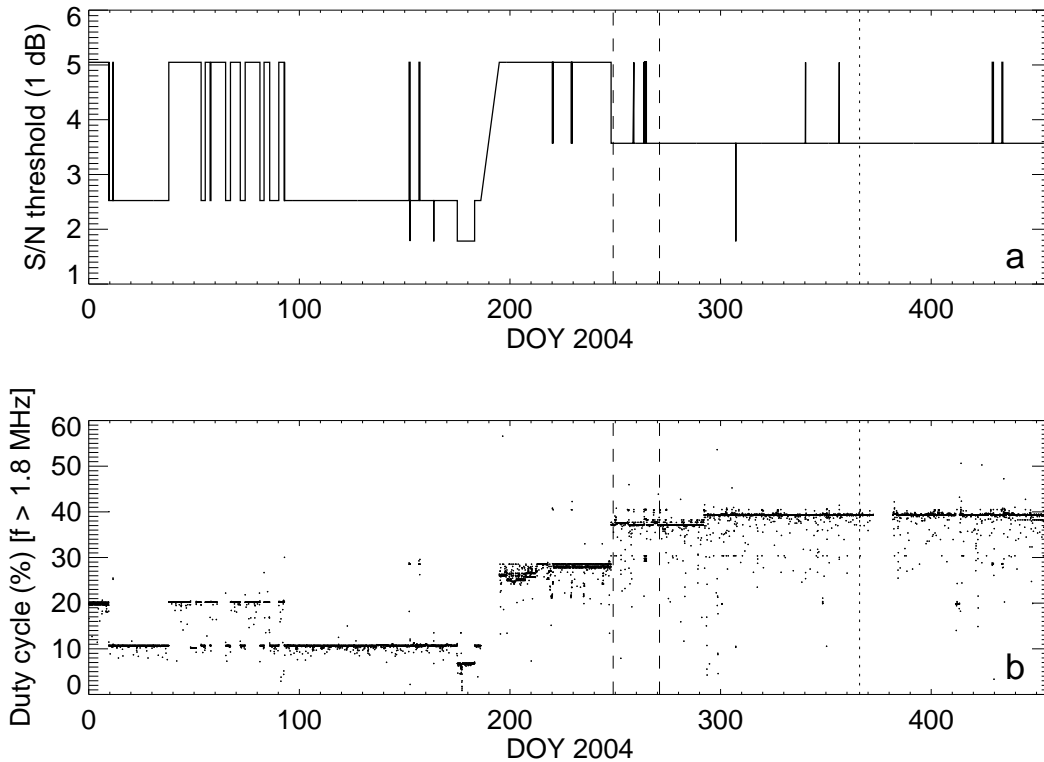


Figure 1: (a) Effective S/N corresponding to a burst detection threshold of 1 dB, versus time, in the high frequency band of the RPWS/HFR. Variations result from the various integration time and channel bandwidth used at different times. (b) HFR duty-cycle spent above 1.8 MHz. Dashed vertical lines delimitate the period of September 2004 studied in more details in this paper. The dotted vertical line marks 2005/01/01.

of events detected during the very active storm that took place from September 5th to 27th, 2004 (DOY 249 to 271). The detection threshold was quasi-steady at $S/N \sim 3.6$. The top panel shows the integrated occurrence per 15 min. intervals, which reveals a prominent periodicity of recurrence of the events (the computed period is 10h 40min, slightly shorter than the Saturn Kilometric Radiation period of 10h 45.75min measured

by Cassini [Gurnett et al., 2005]). The bottom panel shows individual events in the t - f plane. These observations are consistent with a single storm system located at a latitude about 35° S, where the so-called ‘dragon storm’ was observed at the same time by the Imaging Science Subsystem on Cassini [Porco et al., 2005; Desch et al.]. The radio source rotates with Saturn’s atmosphere and bursts are observable once per turn during ‘episodes’ lasting for about half a rotation. Porco et al. [2005] noted a puzzling phase shift between the visible cloud and the radio burst episodes, the latter occurring on the average ~ 0.2 Saturn rotation earlier than the former. Either the radio bursts must be produced some 70° ahead of the visible cloud, or they must be able to propagate from up to 70° beyond the horizon to Cassini. We propose elements for a solution below. Lightning

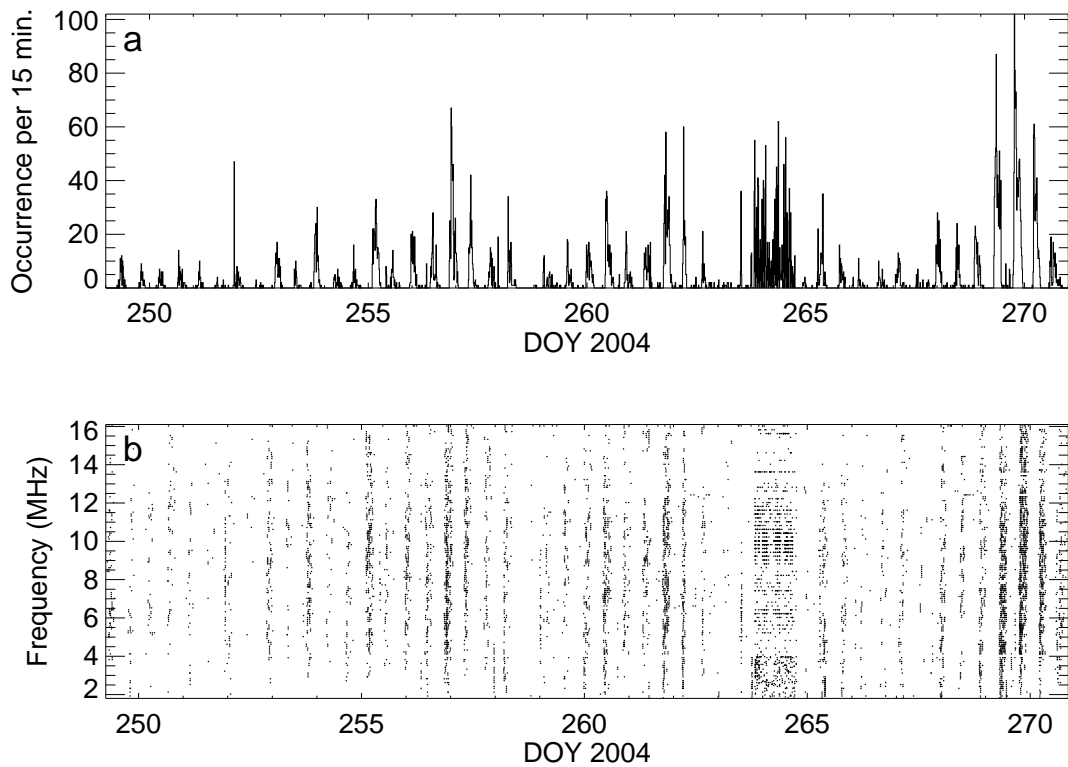


Figure 2: (a) Burst occurrence per 15 min. intervals above a detection threshold of 1 dB, in September 2004. (b) Corresponding distribution of individual bursts versus time and frequency. Bursts are grouped in episodes of ~ 5 hour duration, recurring at 10h 40min intervals.

occurrence is clearly very variable at timescales of days, revealing storm activity much more variable than at the time of both Voyager spacecraft [Zarka, 1985b], with sometimes totally missing episodes (e.g. on DOY 258). This occurrence variation is not due to the spacecraft-source distance, which remained between 125 and 150 R_S over the whole interval ($1 R_S = \text{Saturn's radius} \sim 60300 \text{ km}$). An excess of spurious bursts is detected around DOY 264, related to an instrument setup change. The actual occurrence rate can be derived from the apparent one of Figure 2a via the HFR duty-cycle spent above 1.8 MHz, as plotted on Figure 1b. For the period studied here, this duty-cycle is quasi-permanently about 37%. The ~ 4100 events detected above 1 dB on Figure 2 (excluding

those on DOY 264) translate thus in ~ 11000 actually emitted. The peak detection rate at ~ 80 events per 15 min. corresponds to one lightning flash produced every 4 sec, comparable to the occurrence rate derived by Voyager 1 at Saturn [Kaiser et al., 1983; Zarka and Pedersen, 1983]. The average rate, ~ 4 times lower, is comparable to that of Voyager 2 epoch.

To study in more detail the occurrence of events during an episode, we stacked on Figure

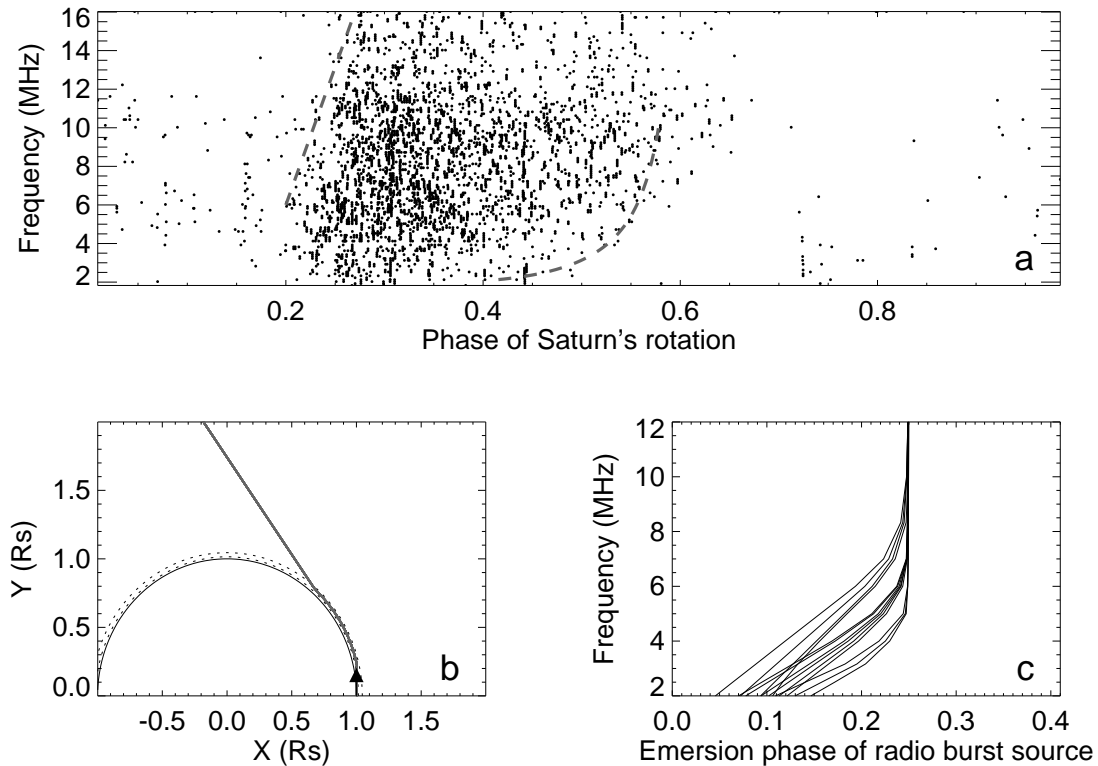


Figure 3: (a) Stacked episodes of Fig. 2b versus phase (with an arbitrary origin). The apparition and disappearance of bursts is frequency-dependent, as outlined by the grey dashed lines. The right one results from computation of the frequency cutoff $f_c = f_{\text{pe-peak}} / \cos \theta$ with θ the angle of incidence of radio waves on Saturn's ionosphere and $f_{\text{pe-peak}}$ taken equal to 2 MHz in Saturn's dayside ionosphere. (b) Example of deviation of a horizontal ray (arrow) at 2 MHz propagating through a model ionosphere (sketched by the dotted lines, with $f_{\text{pe-peak}} = 1$ MHz and located at $1.03 \pm 0.006 R_S$) with a density decrease versus LT of $0.17 \times f_{\text{pe-peak}}$ per hour. The overall ray deviation is 35° . (c) Parametric study of ray deviation over the planet's limb versus frequency, due to radio wave refraction through Saturn's ionosphere. Emersion at the limb in the absence of propagation effect is at phase 0.25. The ionosphere is modelled as a Gaussian layer centered on $R=1.03$ or $1.05 R_S$, with 1σ thickness of 0.003 or 0.006 R_S , and a peak plasma frequency $f_{\text{pe-peak}} = 1., 1.5, \text{ or } 2. \text{ MHz}$, linearly decreasing of 0.13, 0.15, or $0.17 \times f_{\text{pe-peak}}$ per hour of LT.

3a all the episodes of Figure 2b versus phase within Saturn's rotation. Both the apparition and disappearance of bursts seems to be frequency-dependent: lower frequencies start earlier than higher ones, and also stop earlier. Cassini was placed about 06:00 LT (05:55 to 06:30) during the entire interval studied, so that it could see the storm system emerge from Saturn's nightside and disappear under the dayside ionosphere. At disappearance,

the path from the source to the spacecraft crosses the ionosphere at an angle \approx equal to the storm longitude minus the spacecraft longitude ($\Lambda_{\text{storm}} - \Lambda_{\text{s/c}}$), so that radio waves sustain a low frequency (LF) cutoff at $f_{\text{pe-peak}}/\cos(\Lambda_{\text{storm}} - \Lambda_{\text{s/c}})$, plotted as the grey dashed curve on the right of Figure 3a. Let us remind that this cutoff results from reflection of radio waves coming from the atmosphere (where the radio refraction index is $\mu \simeq 1$) and entering the ionospheric plasma slab with peak plasma frequency $f_{\text{pe-peak}}$ (where the refraction index for a wave frequency f is: $\mu = (1 - f_{\text{pe-peak}}^2/f^2)^{1/2}$). This can explain (at least qualitatively) the frequency-dependent radio burst occurrence at the end of episodes [see also Zarka, 1985a]. The frequency-dependent apparition of the bursts (on the left of 3a) is more puzzling. We suggest that it is also due to a propagation effect, but this time through Saturn's nightside ionosphere. The proposed effect comes from the refraction sustained by radio waves with frequency slightly above the cutoff: when it enters the ionosphere, the wave is refracted away from the normal to the plasma layer, and then back towards it when it exits. For a plane plasma slab, the net ray deviation is zero, but not for a spherical layer. The effect is dominant for rays entering the ionosphere at large angle from its local normal. Thus, we studied with 2D ray-tracing the propagation of rays launched horizontally from the storm source through an ionospheric layer with a Gaussian profile around a peak plasma frequency $f_{\text{pe-peak}} \approx 1$ MHz. If the ionosphere has spherical symmetry (i.e. no local time variation of its density) then the ray is either slightly deviated behind the limb (by $\leq 1^\circ$, above a critical frequency equal to a few times $f_{\text{pe-peak}}$) or trapped under the ionospheric layer (below that frequency). However, if we introduce a decrease of the ionospheric electron density (and thus of $f_{\text{pe-peak}}$) versus local time in the nightside hemisphere, as can be expected from gradual recombination (see Figs. 6 and 7 of [Moore et al., 2004] for Saturn's case, and e.g. [Maruyama, 2002] for the Earth's case), then rays can escape the ionospheric layer after temporary trapping, and thus experience an overall deviation of several degrees to several tens of degrees, as sketched in Figure 3b. This effect is stronger at lower frequencies (closer to $f_{\text{pe-peak}}$). Figure 3c shows a series of results obtained by varying the ionospheric model parameters (average altitude and width of the Gaussian ionospheric layer, $f_{\text{pe-peak}}$, and density decrease rate versus LT), where the ray deviation is translated in emersion phase of the radio burst source versus frequency, over the planet's limb (located at phase 0.25). Although not accurately matching the observed emersion profile of Figure 3a, these curves obtained for a reasonable range of ionospheric parameters predict an effect consistent with the one observed, qualitatively as well as in order of magnitude. The above two propagation effects taken together can help solving the discrepancy between the radio burst occurrence and the visible cloud longitude mentioned earlier because they result in an overall phase shift of the radio burst occurrence of the order of 0.1 rotation. Future detailed modelling may further improve the fit. Supporting the importance played by ionospheric propagation effects, we observed that the measured flux of lightning radio bursts is strongly attenuated (by a factor ~ 5) at both episode edges compared to their flux at the center of the episodes.

2 Duration

RPWS/HFR measurements of September 2004 were made with a time constant of 45 msec between consecutively sampled frequencies. Lightning flash duration is directly derived

from the number of consecutive channels in which radio emission is detected. Figure 4 shows the distribution of these durations for events above a detection threshold of 1.5 dB. Flashes last for 1 to 8 consecutive channels, i.e. up to 360 msec. Their distribution is well described by an exponential law $N = N_0 e^{-D/D_0}$ with e-folding time $D_0 = 48$ msec (51 msec for 1 dB threshold). This result is very close to that obtained with Voyager data [Zarka and Pedersen, 1983 ; Zarka, 1985b]. Note that the extended radio spectrum of Saturn's lightning (see below) implies that each flash probably consists of multiple short strokes, like terrestrial flashes [Farrell, 2000].

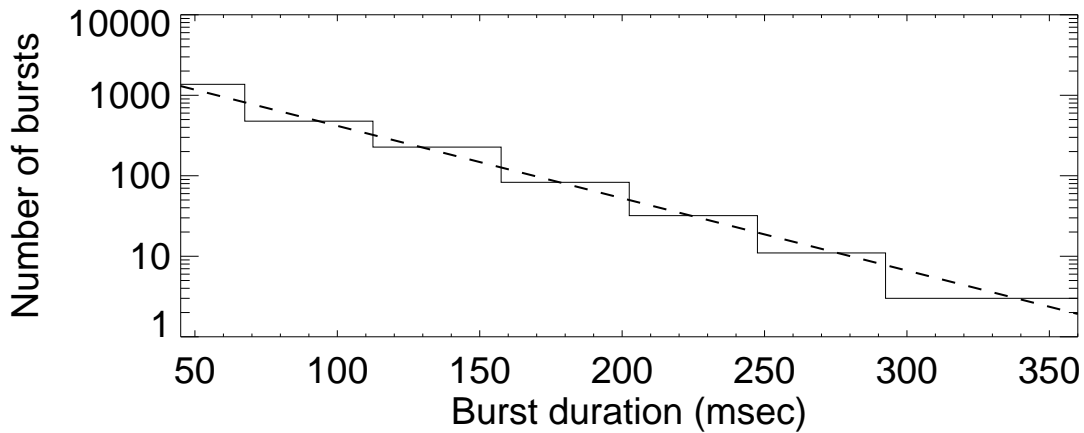


Figure 4: Distribution of burst durations above a detection threshold of 1.5 dB, and fit by an exponential law with e-folding time = 48 msec (51 msec for 1 dB threshold).

3 Lightning flux density and spectral power

Applying the absolute flux density calibration described by Zarka et al. [2004a], which relies on measurement by RPWS/HFR of the galactic background and careful estimation of the receiver background, we obtain the calibrated flux density S of each detected burst (with an estimated accuracy better than $\sim 50\%$). Under the assumption of an isotropic emission, we derive the spectral power of the bursts $P = S \times 4\pi R^2$ with R the spacecraft-source distance, taken here equal to the spacecraft-planet distance. Figure 5a shows the distribution of burst spectral power for the episodes of September 2004. The average spectrum is overplotted as a boldface line, and the average $+1\sigma$ (computed from the spectral power histogram at each frequency) as a lightface line. As with Voyager measurements, the spectrum is found to be nearly flat in the range 2-16 MHz, with an average power of ~ 100 W/Hz, thus a total power $\geq 1.6 \times 10^9$ W per flash. The strongest bursts may exceed 5 times this value. These numbers are within a factor 2 of independent flux and power estimates by Fischer et al. [2006].

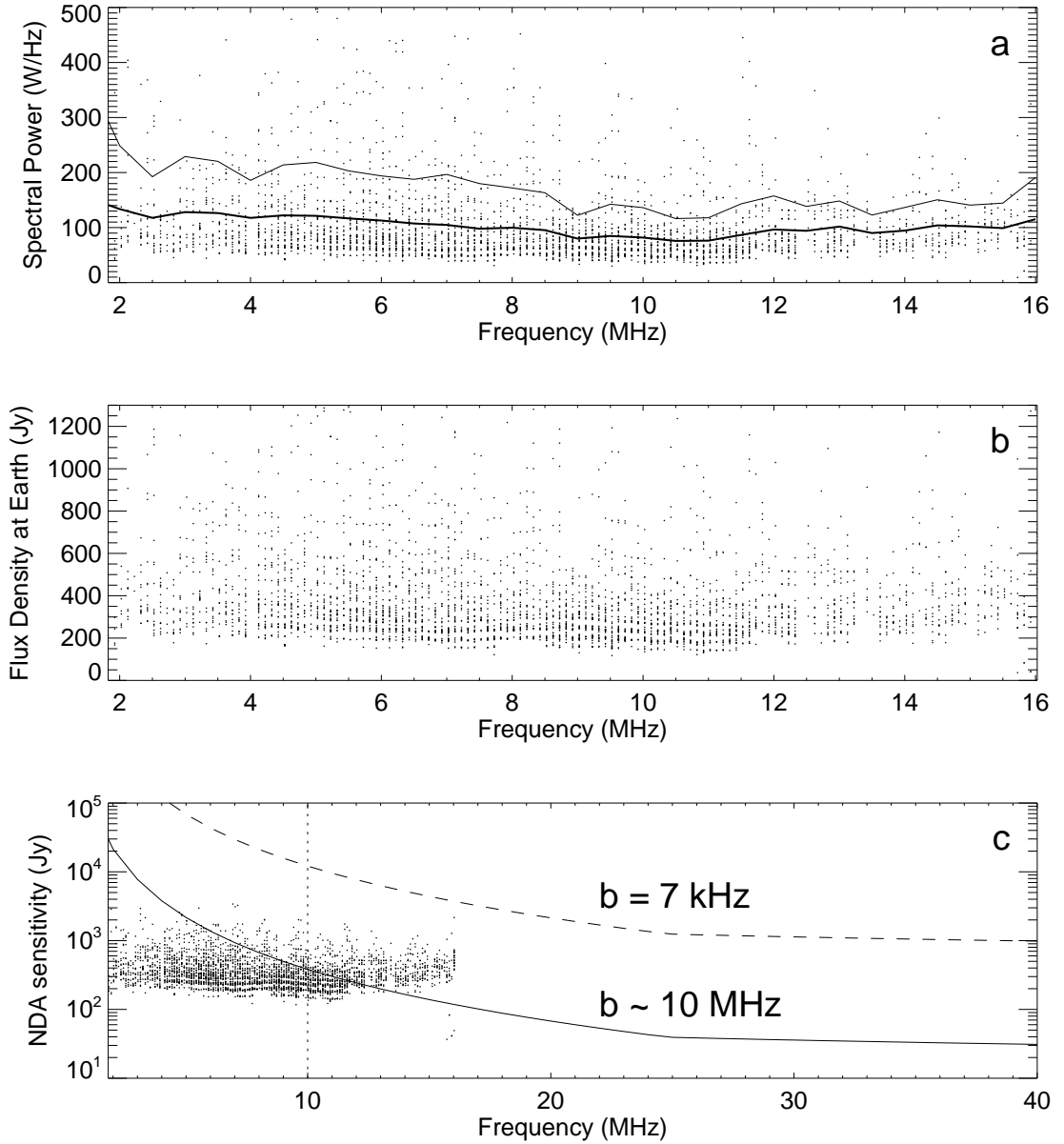


Figure 5: (a) Spectral power versus frequency of September 2004 bursts, average spectrum (boldface line) and average +1 σ (lightface line). The sky background contribution has been subtracted. (b) Corresponding flux densities at Earth ($1\text{Jy} = 10^{-26}\text{Wm}^{-2}\text{Hz}^{-1}$). (c) Same as (b) with different scales, superimposed on the 1σ detection threshold of $\tau = 19$ msec bursts of bandwidth $b = 7$ kHz or 10 MHz with the Nançay Decameter Array (NDA) connected to the R³ receiver (see text). The UTR-2 decameter array in Kharkov would have a detection threshold ~ 1 order of magnitude below NDA for the same b and τ . Earth's ionospheric cutoff is indicated by the dotted vertical line.

4 Ground-based detection

From the above spectral power, the flux density at Earth S_E is deduced as $S_E = P/4\pi R_E^2$ with R_E the Earth-to-Saturn distance, ~ 9.5 AU on average. The flux densities corre-

sponding to Figure 5a are displayed in Figure 5b,c, ranging from ~ 200 to > 1000 Jy ($1\text{Jy} = 10^{-26}\text{Wm}^{-2}\text{Hz}^{-1}$). The possibility to detect these events using a ground-based LF radiotelescope results from the comparison of their flux to the level of sky background fluctuations, which is at 1σ level:

$$\sigma_{\text{sky}} = 2kT_{\text{sky}}/A(b\tau)^{1/2} \quad (1)$$

with A the telescope effective area, b the observation bandwidth, and τ the integration time. The LF sky background temperature can be approximated by:

$$T_{\text{sky}}(\text{K}) \sim 1.15 \times 10^8 / f^{2.5} \quad (2)$$

with $10 \leq f(\text{MHz}) \leq 100$ [van Haarlem et al., 2001]. For the Nançay Decameter Array (NDA) in France, the total area (adding both polarizations together because lightning radio emission is unpolarized) is $A = 48\lambda^2 \leq 7000 \text{ m}^2$.

The resulting sensitivity is plotted versus frequency in Figure 5c for $b = 7 \text{ kHz}$ and $b \sim 10 \text{ MHz}$. The former bandwidth is one typical channel bandwidth of the new Nançay R³ (Robust Radio Receiver of the Nançay Observatory [Weber et al., 2005]), while the latter is its typical total bandwidth (for $2000 \times 7 \text{ kHz}$ channels). With 10 MHz bandwidth, Saturn's lightning should be detectable from Nançay above the Earth's ionospheric cutoff $\sim 10 \text{ MHz}$.

R³ is a digital multichannel spectrograph with access to high (selectable) spectral and temporal resolutions and a large dynamic range. We have performed 5-hour observation runs of Saturn nearly every night from 2004/12/16 to 2005/02/03, with permanent tracking of Saturn, $\tau = 19 \text{ msec}$ time integration and a total band of 14 MHz divided in 2048 channels of $b = 7 \text{ kHz}$ bandwidth. The band $14\text{--}28 \text{ MHz}$ was observed. Data was organized as t-f images of 5000 spectra ($\sim 1.5 \text{ min.}$) $\times 2048$ channels, and processed with a RFI-mitigation software developed in Meudon (RFI = Radio Frequency Interference). The algorithm, which is an improved version of the one described in Zarka et al. [1997], relies upon the fact that with the values of τ and b chosen for the observations, Saturn's lightning radio emissions are much weaker than sky background fluctuations (i.e. $S_E \ll \sigma_{\text{sky}}$). Thus, any pixel with an intensity $\geq 3\sigma_{\text{sky}}$ above the background level is recognized as spurious. An iterative process is applied to compute σ_{sky} in spite of the presence of RFI. Highpass filtering is applied during this process to eliminate slow signal fluctuations due to propagation through the Earth's ionosphere. The spurious pixels recognized by the above method are then masked out, and the remaining 'clean' dynamic spectrum is integrated in frequency over the whole 14 MHz band (equivalent to a $\sim 10 \text{ MHz}$ RFI-free band), and also over the two intervals $14\text{--}21 \text{ MHz}$ and $21\text{--}28 \text{ MHz}$ separately (each equivalent to a $\sim 5 \text{ MHz}$ RFI-free band). This results in three series of integrated intensities versus time ($I_{14\text{--}28}(t)$, $I_{14\text{--}21}(t)$, and $I_{21\text{--}28}(t)$) corresponding to temporal integration $\tau = 19 \text{ msec}$ and effective bandwidth of 5 to 10 MHz . Corrections are applied for the spectral integration over a time variable number of clean channels (within each 19 msec spectrum), and the final time series are normalized by their time variable standard deviation (over each 5000×2048 image). We performed tests suggesting that the algorithm is quite efficient, under the key condition that useful signal is 'hidden' in sky background fluctuations prior

to spectral integration, which is indeed the case for Saturn lightning radio emission as shown in Figure 5b,c.

Unfortunately, Cassini observations revealed that lightning activity on Saturn was very

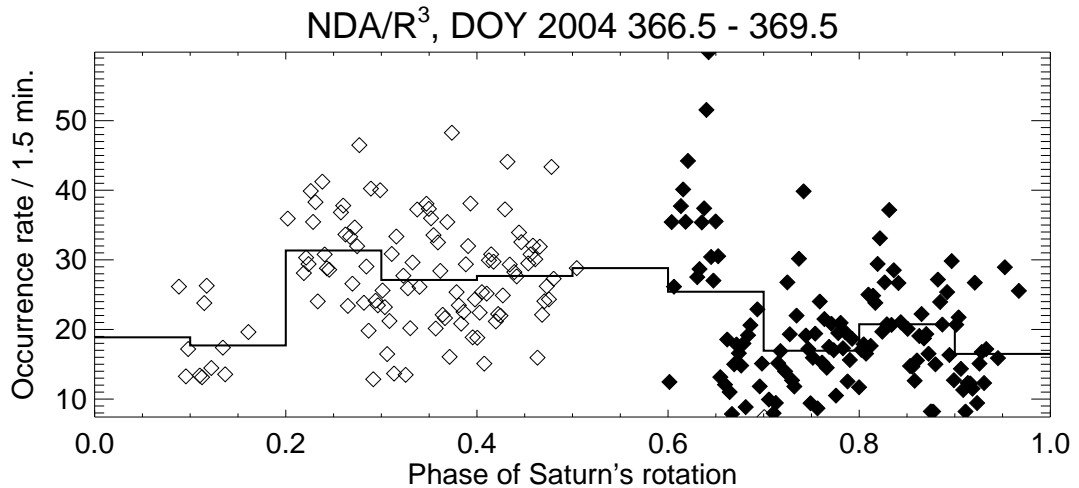


Figure 6: Number of peaks $> 3\sigma$ per 1.5 min. intervals in the 14-21 MHz band detected with the Nançay R^3 receiver during the nights of DOY 366-7 (open diamonds) and DOY 368-9 (filled diamonds), plotted versus phase of Saturn's rotation (arbitrary origin). ~ 7 peaks $> 3\sigma$ per 1.5 min. are expected for pure Gaussian noise. The solid line is the average detection rate over 0.1 rotation bins ($\sim 36^\circ$ or 1 hour). Bins #1 and #6 contain very few observations and are thus subject to a larger error.

low over the interval covered by these first Nançay observations. Close examination of RPWS dynamic spectra and occurrence diagrams suggests possible weak episodes between 2004/12/31 (DOY 2004 366) and 2005/01/03 (DOY 2004 369). Two nights of observations were performed at Nançay on DOY 366-7 and 368-9. Figure 6 shows the number of peaks $> 3\sigma$ counted per 1.5 min. intervals (5000 values) in the time series integrated over the 14-21 MHz band. ~ 7 peaks are expected above 3σ for 5000 samples of pure random (Gaussian) noise. The higher number detected here may be due for a large part to weak residual RFI, and possibly to bursts of Saturnian origin. Direct comparison of Nançay and Cassini data is difficult because of the different local time and distance of the two observers relative to Saturn, Cassini being at 07:25 LT and Nançay at about 12:00 LT (and 67.4 light-minutes farther) on DOY 2004 366-369. Overall occurrence is expected to be shifted by $\sim 5\text{h}42\text{m}$ between Cassini and Nançay, while intense bursts generated when the source is between these two LT might be seen by both observers. Examination of Cassini data suggests that part of the Nançay observation of DOY 366-7 and possibly the start of that of DOY 368-9 may have taken place at the time of Saturnian burst occurrence. On Figure 6, Nançay peak counts are plotted versus phase of Saturn's rotation, in 0.1 rotation bins ($\sim 36^\circ$ or 1 hour per bin). We remark that:

- the two observations sampled distinct phase ranges
- there appears to be an interval of 1-2 bins of low detection rate at the start of the first observation, followed by 3 bins of higher detection rate

- on the second night of observation, 1 ‘high’ bin is followed by 3 ‘low’ bins
- the whole data set organises in ~ 5 consecutive bins of high detection rate and 5 consecutive bins of low detection rate, consistent with observation of a single storm system rotating with the planet.

Although not yet fully conclusive, this result is encouraging.

5 Discussion and Conclusions

This study is still preliminary and a lot more will be done about Saturn’s lightning with RPWS until the end of the Cassini tour. However, the HFR has already proved to be a powerful lightning detector. Lightning radio bursts detected by Cassini have physical properties (short timescale occurrence, duration, flux, spectral power and spectrum shape) similar to those measured by Voyager 1 and 2 a quarter of a century ago. By contrast, the occurrence of lightning is found to be very variable at timescales of days to weeks [see also Desch et al.]. Voyager 2 observed an equatorial storm system similar to that discovered by Voyager 1 nine months earlier, only less well-defined or more spread in longitude. It was interpreted as being possibly the same, long-lasting storm system [Zarka, 1985b]. Cassini observes at intermediate southern latitudes well-defined storm systems appearing suddenly, lasting for days to weeks (during which the lightning source rotates with the atmosphere), with peak occurrence rates as high as 0.25 sec^{-1} , and then disappearing for weeks to months. The observations of September 2004 reveal strong ionospheric propagation effects through both the nightside and dayside ionosphere. The detailed modelling of burst occurrence and intensity versus frequency and geometry of observation should eventually bring new information on Saturn’s ionosphere. But the mere existence of these effects confirms – if it were necessary – the atmospheric origin of the detected radio bursts.

Intense events appear to be detectable from the ground even by medium-size instruments as the NDA (taking advantage of the broad intrinsic bandwidth of the emission and of modern RFI-mitigation capabilities), and a fortiori by larger instruments as the UTR-2 array in Kharkov [Sidorchuk et al.; Zarka et al., 1997] and soon LOFAR [Zarka et al., 2004b]. We have obtained encouraging but not yet conclusive results: high detection rates in Nançay (higher than from the more sensitive RPWS) suggest that only a small fraction of the events detected from the ground may be of Saturnian origin, but these events show a coherent organization versus phase of Saturn’s rotation. This first campaign of ground-based observations took place during a period of low lightning activity on Saturn, and it will be repeated at the next occurrence of intense activity not too far from Saturn’s opposition (daytime observations suffer a too high level of RFI pollution).

We will also attempt to locate directly the instantaneous sources of the most intense bursts (with $S/N > 15 - 20 \text{ dB}$) in the atmosphere using the so-called ‘direction-finding’ capability of RPWS/HFR [see Cecconi et al.]. Finally, a major question to be addressed by RPWS is the existence of Titan lightning. Preliminary analysis of the first 6 Titan flybys between 2004/01/01 and 2005/03/31 did not reveal any strong event. A few flybys were polluted by solar type III emissions, which should be eliminated before searching for

statistical evidence of weak Titan lightning (as $1/R^2$ occurrence or intensity variation). The good sensitivity of RPWS exploited during the 40 Titan flybys to come should allow to answer this question. Besides, study of the radio emission of Saturn lightning is expected to provide significant advances on lightning physics, atmospheric and ionospheric physics, and be an ideal testbed for the validation of LF ground-based observations at high sensitivity.

References

- Cecconi, B., P. Zarka, and W. S. Kurth, SKR polarization and source localization with the Cassini/RPWS/HFR instrument: first results, in *Planetary Radio Emissions VI*, H. O. Rucker, W. S. Kurth, and G. Mann (eds.), Austrian Academy of Sciences Press, Vienna, 2006, *this issue*.
- Desch, M. D., G. Fischer, M. L. Kaiser, W. M. Farrell, W. S. Kurth, D. A. Gurnett, P. Zarka, A. Lecacheux, C. Porco, A. Ingersoll, and U. Dyudina, Cassini RPWS and imaging observations of Saturn lightning, in *Planetary Radio Emissions VI*, H. O. Rucker, W. S. Kurth, and G. Mann (eds.), Austrian Academy of Sciences Press, Vienna, 2006, *this issue*.
- Farrell, W. M., Planetary radio emission from lightning: discharge and detectability, in "Radio Astronomy at Long Wavelength", Geophysical Monograph 119, AGU, 179–186, 2000.
- Fischer G., W. Macher, M. D. Desch, M. L. Kaiser, P. Zarka, W. S. Kurth, W. M. Farrell, A. Lecacheux, B. Cecconi, and D. A. Gurnett, On the intensity of Saturn lightning, in *Planetary Radio Emissions VI*, H. O. Rucker, W. S. Kurth, and G. Mann (eds.), Austrian Academy of Sciences Press, Vienna, 2006, *this issue*.
- Gurnett, D. A., and 29 co-authors, The Cassini Radio and Plasma Wave Investigation, *Space Sci. Rev.*, **114**, 395, 2004.
- Gurnett, D. A., and 27 co-authors, Radio and Plasma Wave Observations at Saturn: Initial Results from Cassini, *Science*, **307**, 1255-1259, 2005.
- Kaiser, M. L., J. E. P. Connerney, and M. D. Desch, Atmospheric storm explanation of saturnian electrostatic discharges, *Nature*, **303**, 50–53, 1983.
- Maruyama, T., Longitudinal peculiarity of topside electron density at 1100 km, URSI proceedings, Maastricht, 8/2002. <http://hawk.iszf.irk.ru/URSI2002/URSI-GA/papers/p1286.pdf>
- Moore, L. E., M. Mendillo, I. C. F. Müller-Wodarg, and D. L. Murr, Modeling of global variations and ring shadowing in Saturn's ionosphere, *Icarus*, **172**, 503–520, 2004.
- Porco, C. C., and 34 co-authors, Cassini Imaging Science: Initial Results on Saturn's Atmosphere, *Science*, **307**, 1243-1247, 2005.
- Sidorchuk, K. M., A. A. Konovalenko, V. N. Mel'nik, H. O. Rucker, G. Fischer, A. Lecacheux, E. P. Abranin, A. A. Stanislavskij, O. M. Ul'yanov, V. V. Zakharenko,

- Search for non-thermal radio emission from planets and stars at decameter wavelengths, in *Planetary Radio Emissions VI*, H. O. Rucker, W. S. Kurth, and G. Mann (eds.), Austrian Academy of Sciences Press, Vienna, 2006, *this issue*.
- Van Haarlem, M. P., and 27 co-authors, LOFAR scientific applications, Report ASTRON-LOFAR-00230, v1.00, 07-03-01, <http://www.lofar.org>, 2001.
- Warwick, J. W., J. B. Pearce, D. R. Evans, T. D. Carr, J. J. Schauble, ; J. K. Alexander, M. L. Kaiser, M. D. Desch, M. Pedersen, A. Lecacheux, G. Daigne, A. Boischot, C. H. Barrow, Planetary Radio Astronomy observations from Voyager 1 near Saturn, *Science*, **212**, 239–243, 1981.
- Weber, R., C. Viou, A. Coffre, L. Denis, P. Zarka, and A. Lecacheux, DSP-enabled Radio Astronomy: Towards IIIZW35 reconquest, *J. Appl. Signal Proc.*, **16**, 1-8, 2005.
- Zarka, P., and B. M. Pedersen, Statistical study of Saturn Electrostatic Discharges, *J. Geophys. Res.*, **88**, 9007-9018, 1983.
- Zarka, P., Directivity of Saturn Electrostatic Discharges and ionospheric implications, *Icarus*, **61**, 508-520, 1985a.
- Zarka, P., Saturn Electrostatic Discharges: characteristics, comparison to planetary lightning and importance in the study of Saturn's ionosphere, in *Planetary Radio Emissions*, H. O. Rucker and S. J. Bauer (eds.), Austrian Academy of Sciences Press, Vienna, 237–270, 1985.
- Zarka, P., J. Queinnec, B. P. Ryabov, V. B. Ryabov, V. A. Shevchenko, A. V. Arkhipov, H. O. Rucker, L. Denis, A. Gerbault, P. Dierich, and C. Rosolen, Ground-Based High Sensitivity Radio Astronomy at Decameter Wavelengths, in *Planetary Radio Emissions IV*, H. O. Rucker, S. J. Bauer, and A. Lecacheux (eds.), Austrian Academy of Sciences Press, Vienna, 101–127, 1997.
- Zarka, P., B. Cecconi, and W. S. Kurth, Jupiter's low frequency radio spectrum from Cassini/RPWS absolute flux density measurements, *J. Geophys. Res.*, **109**, A09S15, doi:10.1029/2003JA010260, 2004a.
- Zarka, P., W. M. Farrell, M. L. Kaiser, E. Blanc, and W. S. Kurth, Study of solar system planetary lightning with LOFAR, *Planet. Space Sci.*, **52**, 1435-1447, 2004b.